The Nansen Environmental and Remote Sensing Center

a non-profit environmental and
climate research institute

Thormøhlens gate 47,
N-5006 Bergen
Norway

**NERSC Technical Report no. 399**

Prepared under the SKD Fast Track Initiative project:
*MUlti-scalar DYnamics of Flood EvEnTs (MUDYFEET)*

# DEVELOPMENT OF AN ATMOSPHERIC RIVER DETECTION ALGORITHM

by

**Stephen Outten**

**Bergen, October 16, 2019**

**Nansen Environmental and Remote Sensing Center**
Thormøhlens gate 47
N-5006 Bergen - NORWAY
Phone: +47 55 20 58 00 Fax. +47 55 20 58 01
E-mail: administrasjon@nersc.no Web.site: http://www.nersc.no

a non-profit environmental and climate research institute

# REPORT

| | |
|---|---|
| **TITLE**<br>Development of an atmospheric river detection algorithm | **REPORT No.**<br>Technical report no. 399 |
| **CLIENT**<br>Bjerknes Center for Climate Research | **CONTRACT**<br>SKD Fast Track Initiative project:<br>*MUlti-scalar DYnamics of Flood EvEnTs (MUDYFEET)* |
| **CONTACT PERSON**<br>Stephen Outten | **AVAILABILITY**<br>Open |
| **AUTHORS**<br>Stephen Outten | **DATE**<br>October 16, 2019 |

## SUMMARY

*This report details the development of an algorithm for automatically detecting and forming tracks for atmospheric rivers (AR) approaching Southern Norway. This algorithm was applied to the latest generation of reanalysis from the European Centre for Medium-Range Weather Forecasts (ECMWF), known as ERA5. The algorithm is used to identify ARs similar to the one responsible for the Voss flooding event in October 2014.*

| | |
|---|---|
| **APPROVAL**<br><br>*Stephen Outten, Lead author* | <br><br>*Sebastian H. Mernhild, Director* |

## TABLE OF CONTENTS

# 1. Background and objectives

Extreme events are often the result of interactions between large-scale atmospheric patterns and local scale features, e.g. orography. Traditional approaches to study extreme events typically focus on the importance of either the large scale (e.g. atmospheric rivers) or local scale dynamics. Multi-scalar dynamics investigates the full range of scales, taking a more holistic approach to studying extreme events. For example, a study [Hughes *et al*., 2014] of atmospheric rivers impinging upon western America showed that while changes in the angle of incidence of the atmospheric rivers resulted in only small changes (~6%) to the precipitation on regional scales, they caused large increases (~30%) in extreme precipitation in individual catchment zones. This was due to the local-scale alignment of the moist air-flow with the slopes of the orography.

Extreme precipitation in western Norway is often associated with the onshore flow of a moist jet of marine air interacting with local orography. One example of this situation is the severe flooding that occurred in the city of Voss, Norway on the 28th of October 2014. A previous study of this event by Pontoppidan *et al*. [2017] suggests that the extreme precipitation was a result of the dynamical interactions between the air mass and the terrain. The working hypothesis of this study is that the atmospheric dynamics across scales are important to the occurrence of such extreme flooding events. Hence, two situations with very similar large-scale meteorological conditions may result in an extreme event in one case but not the other, given small difference in their local-scale conditions. As part of the *MUlti-scalar DYnamics of Flood EvEnTs* (MUDYFEET) project, existing reanalysis was analyzed to identify occurrences of the same large-scale dynamics as occurred during the 2014 flood event in Voss [e.g. NRK 28.10.2014]. Such events may/may not have been accompanied by flooding due to the presence/absence of the local scale interactions. The follow up investigation of these events and their comparison to the Voss extreme flooding event is planned to be carried out by the SKD Extreme Events Team in the Mid-Latitude Dynamics group, under the Global Theme at the Bjerknes Centre. The ***primary objective*** of this part of the work has therefore been to identify occurrences of similar large-scale structures and generate a dataset and analysis of such events to support the ongoing work of the Extreme Events Team.

# 2. Atmospheric river detection

Since the key large-scale feature associated with the Voss flooding event was an atmospheric river (AR), I examined the 40 years available of hourly data of the new generation of ECMWF reanalysis (ERA5) to identify ARs. To achieve this goal, I encoded an algorithm to automatically detect ARs approaching Southern Norway, and to identify the tracks of the cores of those ARs, based on the methods of Lavers *et al.* [2012] and Brands *et al.* [2017]. The algorithm analyses the integrated water vapor data in the reanalysis and produces a table containing all of the times an AR is identified, along with its length, longitudinal extent, integrated vapor transport along its core, and the coordinates of the track through the core of the river at that time. This information can not only be used for statistical analysis of ARs approaching Southern Norway over the last 40 years, as found in ERA5, but is also sufficient to extract a small subset of the reanalysis containing only AR events, for any relevant fields of interest.

The algorithm employed works solely on analyzing the integrated vapor transport (IVT). An overview of the algorithm is given in Figure 1. A boundary line is defined off the coast of Norway. This is positioned off the coast so as to ensure a clear identification of the AR before it has a chance to interact with the orography, which will make identification far more complex. At each time in the data, the IVT is checked along this boundary. If it exceeds a trigger threshold, $P_1$, then an AR has potentially been detected. In this case, the grid point on the boundary line with the maximum IVT is identified, along with the direction of IVT at this point. This is considered to be the end of the AR closest to Norway.

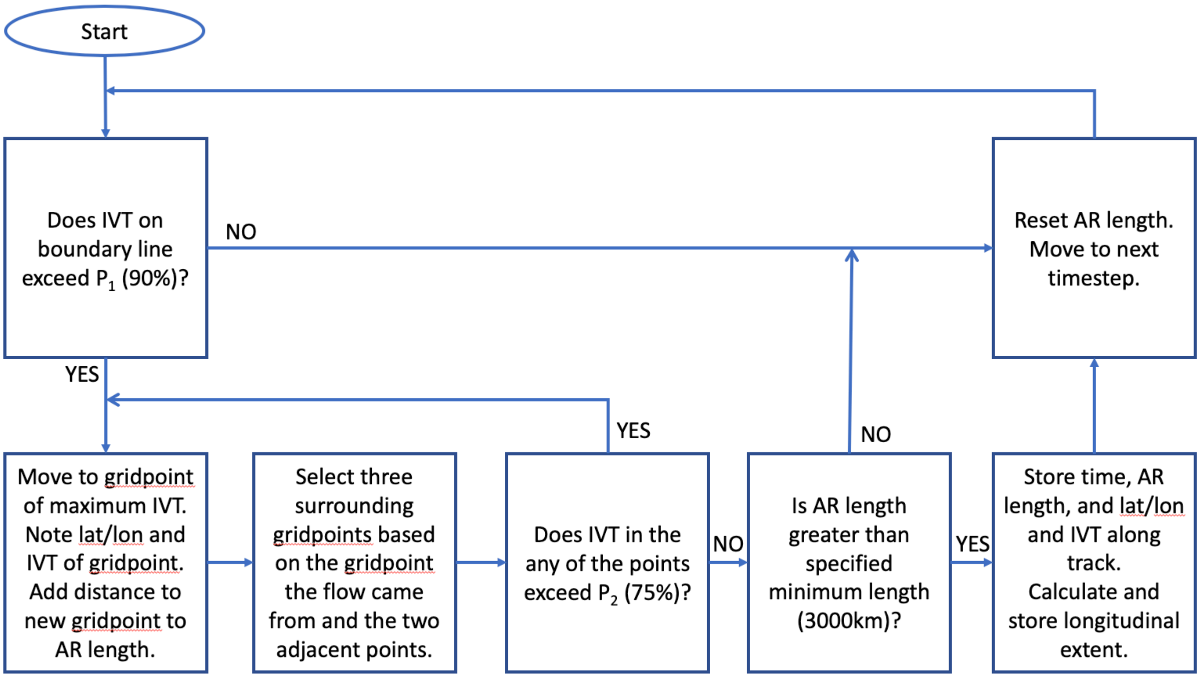


**Figure 1: Flowchart of algorithm for identifying track of AR based on IVT.**

The direction of the flow is converted into one of the eight cardinal directions, thus allowing it to be tracked back to the surrounding grid point from which the flow came, along with the two grid points in cardinal directions on either side of it. For example, if the flow in the original grid point was found to be from the southwest, the algorithm would now examine the grid points to the west, southwest, and south. The grid point from these three points with the maximum IVT is then selected and compared to the tracking threshold, $P_2$. If the IVT exceeds the threshold, the algorithm moves to this point and repeats the process; identifying three grid points from which the flow may have come, taking the point with the maximum IVT, and comparing it again to the tracking threshold, $P_2$. The distance from each grid point to the next is calculated and summed throughout the process. The algorithm continues in this way until it finds locations where the IVT is less than the tracking threshold, which defines the end of the AR tack. If the total length of the AR track is greater than a length criteria, here I use 3,000 km (based on Brands *et al.*, 2017), then the algorithm stores the latitude and longitude of each grid point of the track, along with the IVT of each point and the total length of the AR track. The algorithm then moves on to the next time in the dataset and begins anew. An example AR track from the start of the Voss event at midnight on 26$^{th}$ October 2014 is shown in Figure 2.

Since there is no well-established threshold of IVT for AR occurrence, Lavers *et al.* [2012] proposed that the thresholds should be based on percentiles of the IVT, hence the nomenclature of $P_x$ used here. In this work, the trigger threshold, $P_1$, is set to the 90$^{th}$ percentile, while the tracking threshold, $P_2$, is set to 75$^{th}$ percentile. These values were selected based on the investigation of different possible values conducted by Brands *et al.* [2017]. IVT climatologies change both by location and season, therefore the IVT percentiles are calculated at each grid point and for each month separately.

26-10-2014 00 hrs

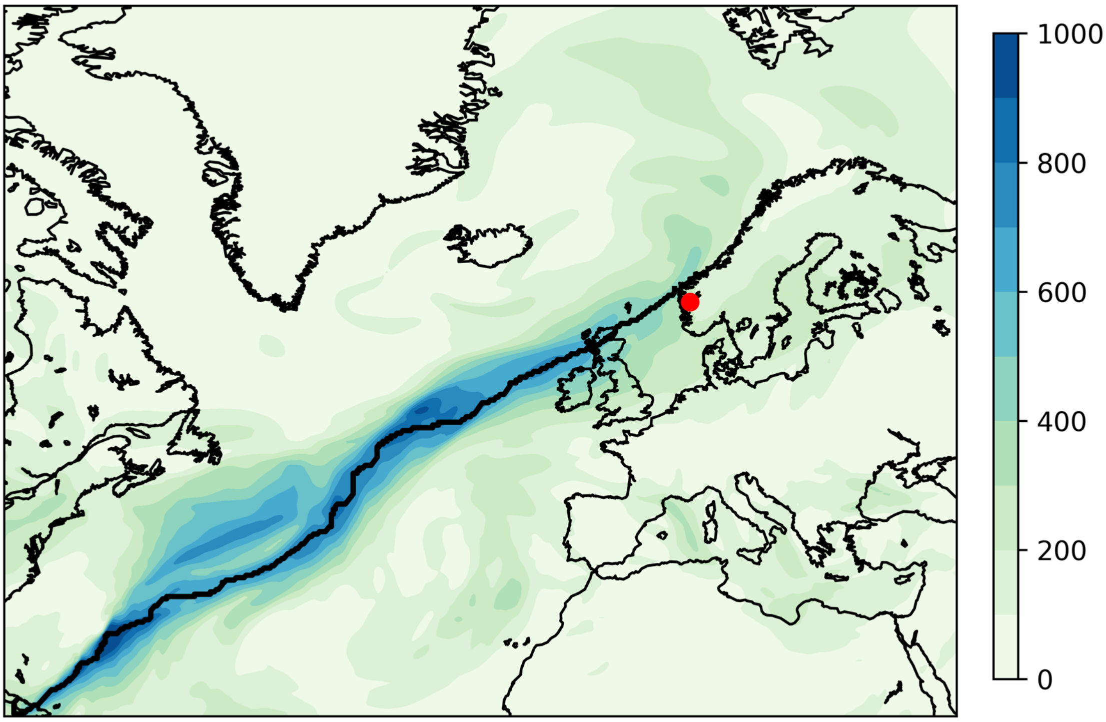


**Figure 2: Integrated vapor transport for atmospheric river at the start of the Voss flooding period, along with the track produced by the algorithm. Units are kg m$^{-1}$ s$^{-1}$. The red dot shows the location of Voss.**

A further criterion for AR identification is the persistence of an AR over time. Once all instantaneous times with an AR occurring have been identified, I combine those ARs which are not separated by at least 24 hours and remove those ARs which do not persist for at least 18 hours. These "persistence" criteria were proposed by Lavers *et al.* [2012]. This produces the final list of ARs identified in the ERA5 reanalysis. In previous works, the length criteria was taken as a longitudinal extent, i.e. the distance from the longitude of one end of the AR to the longitude of the other end. My algorithm also calculates and stores this information so the resulting identified ARs could be reduced further with this as a criterion if so desired.

In summary, the algorithm identifies the tracks based on maximum IVT and the direction of flow of IVT at every time in the hourly ERA5 dataset, where the grid point on the offshore boundary line exceeds the 90$^{th}$ percentile of IVT and each point on the resulting track exceeds the 75$^{th}$ percentile of IVT, as calculated separately by grid point and month. It includes only those ARs with a total length of the track greater than 3,000 km, and which persist for more than 18 hours. The algorithm then stores the IVT, latitude and longitude of each point along each track, as well as the time of occurrence, the total length, and the longitudinal extent. The algorithm has been setup such that all of the thresholds and criteria used can be easily changed and the algorithm quickly rerun.

## 3. Atmospheric rivers similar to Voss ARs

The purpose of this work has been to identify ARs which are similar to that associated with the Voss flooding event of 2014, and to create a small dataset which contains a subset of the ERA5 reanalysis for variables of interest, such as IVT, mean sea level pressure, precipitation, wind, etc., when similar ARs are occurring. To achieve this, the algorithm was run against the complete 40 years of IVT hourly data in ERA5, spanning the period from 1979 to 2018. The identified AR tracks for the Voss period from 26th October 2014 until 29th October 2014 were isolated. These were each compared to all other ARs identified in ERA5, and similar ARs were identified based on four criteria. These criteria were;

1) the ARs must end in the same grid point (i.e. have the same point on the boundary line off the coast of Norway),
2) they must have similar IVT in the end grid point of the AR,
3) they must have similar total lengths,
4) they must not have large mean deviations in position from the original Voss AR they are compared to.

The first two criteria ensure that approximately the same vapor is being transported to the same location off the coast of Norway. The second two criteria ensure that the AR is similar in length and position to the Voss AR it is compare with. The fourth criteria was obtained by calculating the distance between each point on the tested AR and its equivalent point on the Voss AR it was being compared to, i.e. the distance from first point on the track of the tested AR to first point on the Voss AR, then the distance of the second point to the second point, etc. The mean of these distances thus provided a measure of the deviation of the location of the tested AR from the comparative Voss AR.

| Voss AR time | Similar AR time | Voss AR length (km) | Similar AR length (km) | Length diff. (km) | Voss IVT at end (kg $m^{-1}$ $s^{-1}$) | Similar IVT at end (kg $m^{-1}$ $s^{-1}$) | IVT diff. at end (kg $m^{-1}$ $s^{-1}$) | Mean deviation (km) |
|---|---|---|---|---|---|---|---|---|
| 2014-10-26:14 | 2015-02-19:02 | 9468 | 9797 | 329 | 557.9 | 557.5 | 0.40 | 422 |
| 2014-10-26:15 | 1997-08-21:11 | 9900 | 9492 | -408 | 575.4 | 575.0 | 0.41 | 494 |
| 2014-10-27:13 | 2003-01-26:22 | 3309 | 3375 | 66 | 666.4 | 666.9 | 0.51 | 444 |
| 2014-10-27:19 | 1990-02-24:01 | 3617 | 3997 | 380 | 605.9 | 605.3 | 0.63 | 390 |
| 2014-10-26:06 | 2002-04-22:05 | 9533 | 9383 | -150 | 563.0 | 561.3 | 1.66 | 482 |
| 2014-10-27:20 | 1989-02-06:13 | 3657 | 4100 | 444 | 643.5 | 645.7 | 2.20 | 428 |
| 2014-10-27:10 | 1989-10-16:13 | 3251 | 3186 | -65 | 641.6 | 644.5 | 2.92 | 194 |
| 2014-10-27:10 | 1996-02-15:18 | 3251 | 3114 | -137 | 641.6 | 645.7 | 4.13 | 496 |
| 2014-10-27:12 | 2018-08-15:23 | 3194 | 3626 | 432 | 668.9 | 673.1 | 4.26 | 475 |
| 2014-10-26:01 | 2007-08-03:23 | 9710 | 9419 | -291 | 460.9 | 456.6 | 4.33 | 384 |
| 2014-10-27:20 | 1989-02-06:15 | 3657 | 3880 | 223 | 643.5 | 638.8 | 4.61 | 427 |
| 2014-10-27:19 | 1989-02-06:18 | 3617 | 3652 | 35 | 605.9 | 611.1 | 5.26 | 400 |
| 2014-10-27:10 | 1994-12-11:18 | 3251 | 3100 | -151 | 641.6 | 636.2 | 5.44 | 294 |
| 2014-10-27:18 | 1989-02-07:00 | 3720 | 3440 | -280 | 588.6 | 594.1 | 5.51 | 334 |
| 2014-10-26:02 | 2002-04-22:07 | 9764 | 9658 | -107 | 496.6 | 502.3 | 5.73 | 472 |
| 2014-10-26:05 | 1999-12-24:04 | 9613 | 9405 | -208 | 549.4 | 543.0 | 6.38 | 477 |
| 2014-10-27:18 | 1983-10-12:20 | 3720 | 3338 | -381 | 588.6 | 595.3 | 6.66 | 251 |
| 2014-10-26:18 | 1996-11-03:05 | 9440 | 9338 | -102 | 640.2 | 633.3 | 6.88 | 412 |
| 2014-10-26:00 | 1986-03-22:08 | 10005 | 9951 | -54 | 443.4 | 435.8 | 7.61 | 380 |
| 2014-10-26:02 | 1986-03-22:11 | 9764 | 9542 | -223 | 496.6 | 488.8 | 7.73 | 388 |
| 2014-10-27:18 | 1989-02-06:23 | 3720 | 3383 | -337 | 588.6 | 597.8 | 9.17 | 320 |

**Table 1: ARs similar to Voss ARs based on difference in length, difference in IVT in end grid point closest to Norway and mean of distance between points along their tracks. The AR comparison shown in Figure 3 and Figure 4 is highlighted in Green.**

A range of values for the criteria were tested so as to reduce the number of ARs to a small group. The final values used were an IVT difference of less than or equal to 8 kg $m^{-1}$ $s^{-1}$ in the end grid point, a difference in length of less than or equal to 500 km, and a mean difference in track locations of less than or equal to 400 km. These criteria reduced the total number of instantaneous ARs to twenty-one, as shown in Table 1.

A dataset has been created where variables of interest have been extracted from ERA5. Since the resulting dataset was not excessive in size, the variables were extracted for all of the ARs identified by the algorithm, not just the reduced list shown in Table 1. The variables extracted include mean sea level pressure (MSLP), precipitation, and of course, IVT. Other fields can easily be added to this list and the extraction redone, or the extraction could quickly and easily be redone with a smaller subset of selected ARs if so desired. This has produced a dataset identifying periods where the large-scale situation was similar to that of the Voss flooding event. These data will be used by the SKD Extreme Events Team to investigate and identify other possible extreme precipitation events in Southern Norway.

To show the results of the implemented method of comparison, Figures 3 and 4 show comparisons of the IVT and MSLP for the AR occurring on 6th February 1989 at 18hr, compared to the AR occurring during the Voss event on 27th October 2014 at 19hr. This comparison is highlighted in green in Table 1.

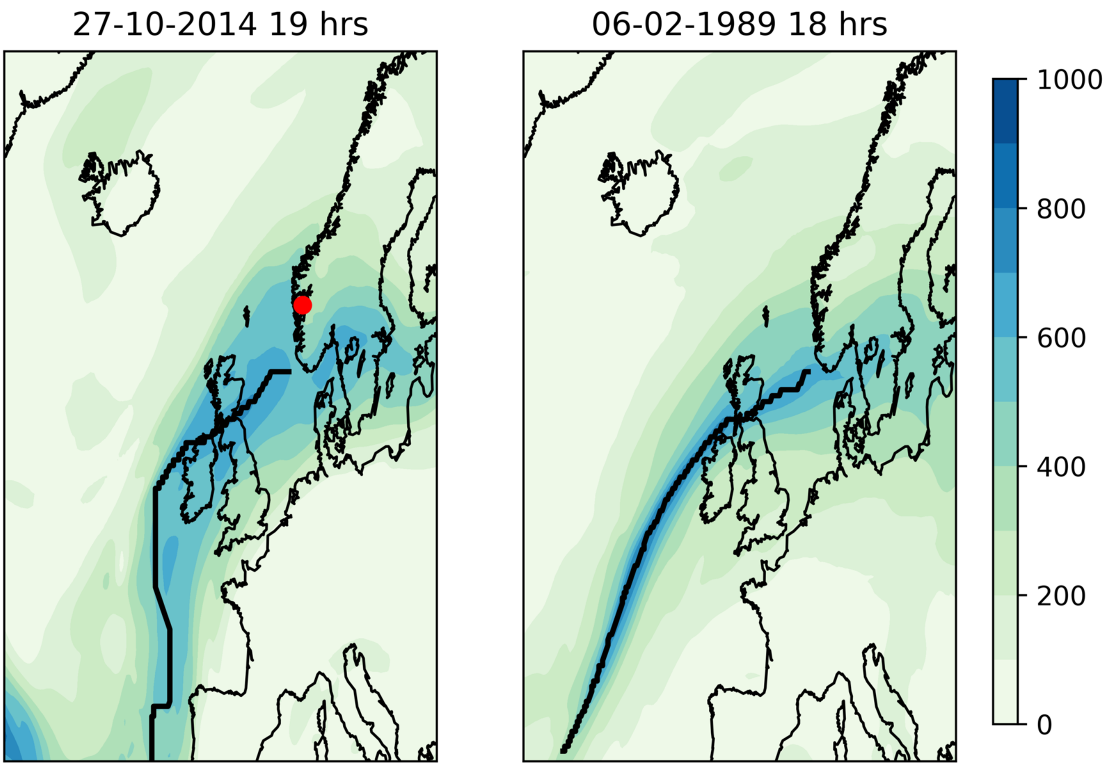


**Figure 3: Comparison of integrated vapor transport and resulting atmospheric river tracks for a time during the Voss event (left) and a similar event in 1989 (right). Units are kg $m^{-1}$ $s^{-1}$. The red dot shows the location of Voss.**

The identified AR tracks are very similar across the U.K. and heading towards Norway. They deviate more upstream where the Voss AR comes from almost directly south while the comparative AR comes from south-south west. This is reflected in Table 1 as the mean deviation between the points along the tracks is around 400 km. From Figure 3 it appears that the difference would be far smaller on the northern end of the AR but far larger towards the southern end. This suggests an improvement in the deviation criteria would prove valuable. However, the IVT along the ARs is very similar, and the comparison in the end grid point closest to Norway is around 606 kg $m^{-1}$ $s^{-1}$ in 2014 compared to 611 kg $m^{-1}$ $s^{-1}$in 1989 This is a difference of less than 1% in IVT.

The comparison of MSLP for the two events is shown in Figure 4. Both situations show a low-pressure band extending northwest across Iceland and towards Northern Norway, with a high-pressure system located over Central Europe. In the situations during the Voss event, the high- and low-pressure centers are located further east and norther east respectively. This accounts for the flow being more curtailed and have a greater meridional component to the west of Central Europe. During the situation in 1989, both the high- and low-pressure centers extend further to the west, hence the upstream end of the jet extending further out into the North Atlantic and coming from the south west instead of the south. One interesting feature of this AR track is that it crosses the isobars at points where there are sharp changes in the directions of the isobars. However, investigating further is beyond the scope of this work.

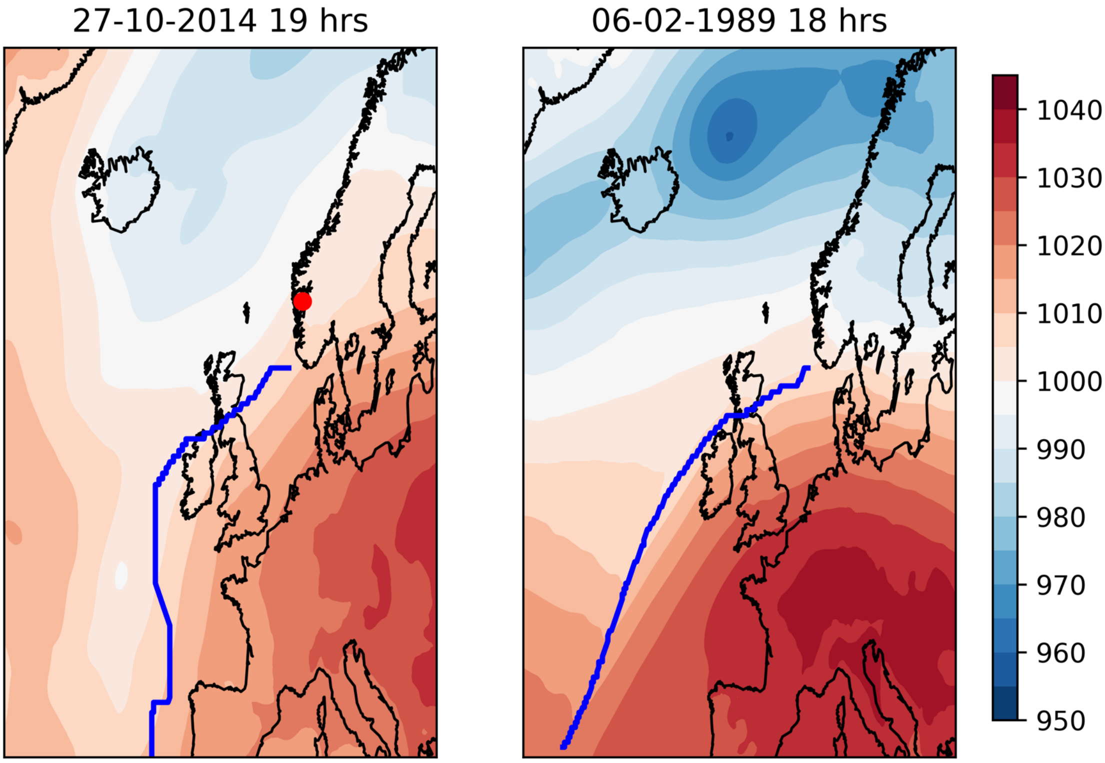


Figure 4: Comparison of mean sea level pressure and the associated atmospheric river tracks for a time during the Voss event (left) and a similar event in 1989. Units are hPa. The red dot shows the location of Voss.

## 4. Summary and future developments

The goal of this work was to identify occasions when the large-scale meteorological situation was similar to that responsible for the Voss flooding event in October 2014. Since the flooding event was strongly connected with the presence of an AR on the large-scale, this work has encoded an algorithm to identify ARs in the ERA5 reanalysis. This has been used to create a dataset of variables of interest such as MSLP and precipitation when these ARs occurred. The identified ARs have been compared to those that occurred during the Voss flooding period to find ARs of similar intensity and structure. The identified Voss-like ARs have been assembled in a dataset that will be used by the Extreme Events Team to select case studies where the large-scale situation is comparable to that which occurred during the extreme precipitation event in Voss, but which did not result in extreme flooding. The dataset created in this work will then form the basis to investigate the selected case studies for the role of multi-scalar dynamics. It remains the ambition of this work that the future analysis by this team will result in a scientific publication and in the longer term contribute to greater understanding of the factors controlling extreme precipitation events.

While the algorithm was not the priority nor a deliverable of the proposed project, it does represent an up-to-date, and flexible tool that could be of use by the research community, including the Extreme Events Team and members of the Hazards theme of the Bjerknes Centre. The codes and dataset are freely available by contacting the author of this report. The algorithm is similar to that proposed by Lavers *et al.* [2012] and Brands *et al.* [2017], with the modification that ARs are selected based on their along-track length instead of their longitudinal extent. Further technical developments have been considered, although time constraints in this project prohibit their development at this time.

The first potential development would be to replace the offshore boundary line with a line generated automatically based on the coastline. This would ensure that the IVT considered for triggering is approximately the same distance from the coast and hence from the effects of the orography. This leads to the second potential development whereby the nearby coast is automatically detected, and the boundary line generated automatically from this. With this development, the user could simply input an approximate latitude and longitude of a locations of interest and the algorithm would identify the nearest coastal grid point, create a boundary line based on the surrounding coastline, and then run the existing algorithm against ERA5. With this development, the algorithm could be used for any location in the world and would provide insights into the effects of ARs on that given location of interest.

Examination of some of the derived AR tracks suggests that the algorithm is only detecting a relatively short distance at the end of the AR and not its entire length. This occurs when there is a strong flow of IVT across the North Atlantic but when there are sections present along its length where the IVT drops below the tracking threshold, $P_2$. A third proposed technical improvement would resolve this issue by incorporating an extra step into the algorithm. The ARs would be tracked using a low value for $P_2$, hence they would capture the entire length of the ARs by accepting the sections of decreased IVT. The extra step would then be added at the end of the algorithm to run through the points along the track and compare them to the higher (current) value of $P_2$. This would result in the algorithm successfully tracking the full length of any AR it identifies, but some tracks will be composed of multiple sections, all of which had IVT meeting the tracking threshold criteria, $P_2$=75%. A similar method has previously been implemented successfully in a tracking algorithm developed by Asgeir Sorteberg.

Beyond the work of the Extreme Events Team to investigate the multi-scalar dynamics of the Voss flooding event, numerous other potential scientific studies are envisioned from this work. The ERA5 reanalysis has only been released this year and is expected to be used in a vast number of studies, including those of precipitation and flooding events. A thorough statistical analysis of the ARs identified in the ERA5 reanalysis would prove extremely useful to many of these future studies, e.g. frequency of occurrence, distribution of intensities, etc. Comparison of such statistics to those based on satellite observations would provide insights into the quality of the ERA5 reanalysis in representing the large-scale transport of moisture by ARs, and thus its usefulness in assessing extreme precipitation events in the many locations where ARs are the dominant factor in such events.

The flexibility of the algorithm allows it to be easily adapted to other datasets. Applying it to the ERA-Interim reanalysis, the precursor to ERA5, would allow an assessment of the improvements of new reanalysis over the old. More valuable though would be its application to the output of climate models, both global and regional. Application to the models of the 6th generation of the Coupled Model Intercomparison project (CMIP6), which are only now becoming available, would allow for an assessment of how well our climate models can simulation ARs. Since ARs are responsible for a large percentage of extreme flooding events across Europe and many parts of the world, the ability of our climate models to accurately reproduce them is of great interest to society and decision-makers alike. Similarly, application to Regional Climate Models and the next generation, so-called 'Global Storm Resolving Models' would provide insights into the ability of these models to accurately assess the impacts of ARs on regional- to local-scales.

Finally, the methodology employed in the algorithm is not the only approach to identifying ARs, and comparisons to other methods may provide insights into future development possibilities. The Norwegian Institute for Air Research (NILU) employs a Lagrangian Particle Dispersion Model (FLEXPART) to calculate the source regions for precipitation of rainfall events. A study comparing the ARs from the tracking algorithm to those identified by the FLEXPART system would serve to assess the strengths and weaknesses of both systems and provide a source of national collaboration between two of Norway's leading institutes. Based on the possibilities discussed here, it is my hope that the AR tracking algorithm developed in this work will prove a useful tool in future research projects.

***Acknowledgements***

This work uses the ERA5 dataset, Copernicus Climate Change Service (C3S) (2017): ERA5: Fifth generation of ECMWF atmospheric reanalyses of the global climate. Copernicus Climate Change Service Climate Data Store (CDS), 14th August 2019. https://cds.climate.copernicus.eu/cdsapp. Thanks to Asgeir Sorteberg for his recommendation for the third technical improvement to the algorithm.

***References***

Brands S., J. M. Gutierrez, and D. San-Martin (2017): 20th-Century Atmospheric River Activity along the West Coasts of Europe and North America: Algorithm Formulation, Reanalysis Uncertainty and Links to Atmospheric Circulation Patterns, *Clim. Dyn.*, **48**, 271-2795

Lavers, D. A., G. Villarini, R. P. Allan, E. F. Wood, and A. J. Wade (2012): The detection of atmospheric rivers in atmospheric reanalyses and their links to British winter floods and the large-scale climatic circulation, *J. Geophys. Res.,* **117**, doi:10.1029/2012JD018027

NRK 28.10.2014: https://www.nrk.no/hordaland/200-ars-flom-pa-voss_-_-ikke-ga-ut-1.12012049